

# The Origin Symphony: Probing Baryogenesis with Gravitational Waves

Yanou Cui,<sup>1,\*</sup> Anish Ghoshal,<sup>2,†</sup> Pankaj Saha,<sup>3,‡</sup> and Evangelos I. Sfakianakis<sup>4,5,6,§</sup>

<sup>1</sup>*Department of Physics and Astronomy, University of California, Riverside, CA 92521, USA*

<sup>2</sup>*Institute of Theoretical Physics, Faculty of Physics,  
 University of Warsaw, ul. Pasteura 5, 02-093 Warsaw, Poland*

<sup>3</sup>*Institute of Particle and Nuclear Studies (IPNS),  
 High Energy Accelerator Research Organization (KEK), Oho 1-1, Tsukuba 305-0801, Japan*

<sup>4</sup>*Texas Center for Cosmology and Astroparticle Physics,  
 Weinberg Institute for Theoretical Physics, Department of Physics,  
 The University of Texas at Austin, Austin, TX 78712, USA*

<sup>5</sup>*Department of Physics, Harvard University, Cambridge, MA, 02131, USA*

<sup>6</sup>*Department of Physics, Case Western Reserve University, Cleveland, OH 44106, USA*

(Dated: December 18, 2024)

Affleck-Dine (AD) baryogenesis is compelling yet challenging to probe because of the high energy physics involved. We demonstrate that this mechanism can be realized generically with low-energy new physics without supersymmetry while producing detectable gravitational waves (GWs) sourced by parametric resonance of a light scalar field. In viable benchmark models, the scalar has a mass of  $\mathcal{O}(0.1 - 10)$  GeV, yielding GWs with peak frequencies of  $\mathcal{O}(10 - 100)$  Hz. This study further reveals a new complementarity between upcoming LIGO-frequency GW detectors and laboratory searches across multiple frontiers of particle physics.

## Introduction.

The origin of the observed matter-antimatter asymmetry  $\eta = \frac{n_b - n_{\bar{b}}}{n_\gamma} \approx 6 \times 10^{-10}$  [1] (in terms of baryon-to-photon ratio) remains a long-standing puzzle in cosmology and particle physics, requiring new physics beyond the Standard Model (SM) to resolve it. Among the solutions proposed for the baryon asymmetry puzzle, Affleck-Dine (AD) baryogenesis [2] is a compelling mechanism where the baryon asymmetry originates from the oscillation and subsequent decay of a baryon-number carrying scalar field. In its original form, the AD mechanism is constructed within the framework of supersymmetry (SUSY) [2–5], where the scalar condensates, potentially essential for baryogenesis, are flat direction moduli fields that are composed of superpartners of the SM quarks/leptons and the Higgs field. These flat direction moduli can generally acquire a large field value displacement during inflation, which spontaneously violates C and CP symmetries, then roll down, oscillate, and decay to baryons in the post-inflationary era. In conventional AD, the scalar field starts to roll and oscillate shortly after the end of inflation, while the inflaton condensate still dominates the Universe before its depletion via reheating [6]. In alternative models, the AD field itself plays the role of the inflaton [7, 8].

Despite the attraction of the AD mechanism, its experimental test is generally challenging due to the high energy scale of the physics involved and the tie to the inflationary era. Fortunately, stochastic gravitational wave background (SGWB) sourced by the AD scalar field provides a new perspective probe by utilizing the naturally

high-energy environment in the early cosmos when the AD mechanism operates. As the AD scalar condensate rolls toward its true vacuum and oscillates around it, it can lead to an era of rapid, non-perturbative particle production (e.g., [9–13]), known as *parametric resonance*, and subsequent fragmentation, which can generate SGWB due to the large, time-dependent field inhomogeneities [14–17] produced therein. In the conventional SUSY-based framework, it was shown that parametric resonance of the AD condensates enabling baryogenesis cannot generate detectable GWs [18–20] [21]. On the other hand, Q-balls, generically predicted in SUSY AD models, may result in a period of early matter domination (EMD) that induces GWs at *second order* through enhancing pre-existing primordial curvature perturbations. [22, 23]. The Q-ball enhanced GW amplitude strongly depends on the speed of the transition from MD to RD [22], with an upper limit given by the commonly used abrupt transition.

The purpose of this work is two-fold: first, we present non-SUSY realizations of the AD mechanism that involve new physics below the electroweak scale and can operate in cosmic epochs long after inflation; second, demonstrate that parametric resonance sourced by AD condensates in such models naturally produces SGWB within reach of upcoming GW experiments. In particular, based on benchmark models with simple renormalizable scalar potentials, we show that in the viable parameter ranges for baryogenesis, parametric resonance of the AD condensate generates GWs with a peak frequency in the range of  $\mathcal{O}(10 - 100)$  Hz, which can be explored by a combination of upcoming detectors, including Cosmic Explorer

(CE) [24] and Einstein Telescope (ET) [25], as well as DECIGO [26] and Big Bang Observatory (BBO) [27] (to capture the lower frequency tail).

The first discovery of GWs by the LIGO-Virgo-KAGRA collaboration [28–30] ushers in a new era of GW astronomy, followed by the more recent compelling evidence of SGWB identified by pulsar timing array (PTA) observations [31–38]. This study uncovers a generic class of well-motivated sources of SGWB, making a timely complement to the literature. The study also reveals a new potential synergy between GW detection and laboratory experiments at energy, intensity, and neutrino frontiers, such as LHC, DUNE, SHiP, FASER [39–46]: interactions between the AD scalar  $\Phi$  and the SM particles are necessary to transfer the asymmetry from the  $\Phi$  field to SM baryons, while the characteristic new physics scale in the AD scalar sector is of  $\mathcal{O}(0.1)$ – $\mathcal{O}(10)$  GeV for viable models with detectable GW frequencies.

The rest of the *Letter* is organized as follows: in the next section, we present the benchmark models and the prediction for the baryon asymmetry; following that, we show the results of lattice simulation for GW signals from these models. Finally, we conclude with an outlook.

## Benchmark Models.

### I. AD scalars: background dynamics and asymmetry generation

We consider a complex scalar field  $\Phi$ , which is a SM gauge singlet with canonical kinetic terms and Einstein gravity. We work with a simple renormalizable polynomial potential:

$$V(\Phi) = \lambda_\Phi |\Phi|^4 + m_\Phi^2 |\Phi|^2 - A(\Phi^n + \Phi_*^n), \quad (1)$$

with  $n$  in principle being any integer  $\leq 4$ . We choose  $n = 2$  for concreteness; however, the results are not expected to change significantly with other choices for  $n$ . The first two terms manifest a  $U(1)$  symmetry, which is broken by the third term as necessary to generate the  $\Phi$ - $\Phi^\dagger$  asymmetry, which later transfers to the baryon asymmetry. We consider the general possibility that  $\Phi$ , as a light spectator field during inflation, starts with a very large (even Planckian) field displacement [47–51], e.g., simply by initial condition, or by quantum fluctuation in the inflationary de Sitter space. We have taken into account the isocurvature constraints from CMB data, which is relevant to light spectator fields in general, and found that they can be generally satisfied (see Section B of the Supplemental Material for details). We denote the typical value at the end of inflation as  $\Phi_{\text{in}}$ , the initial value for our calculations [52]. As long as the (radial) field is light,  $H \gg H_{\text{osc}} \simeq \sqrt{V_{,|\Phi|}/|\Phi|}$ , where  $H_{\text{osc}}$  is the effective mass of  $\Phi$  [48], it remains frozen [53]. The initial phase angle of  $\Phi$ ,  $\theta = \text{Arg}(\Phi)$ , is also set as  $\theta_{\text{in}}$  at the end of inflation

in our observable patch of the universe. As the universe expands, the Hubble rate drops, and at  $H \simeq H_{\text{osc}}$  the field starts rolling. For our parameters, the rolling starts during the radiation-dominated (RD) era, well after the end of inflation.

We analyze the motion of  $\Phi$  in terms of its real and imaginary parts (as defined in  $\Phi = \frac{1}{\sqrt{2}}(\phi_R + i\phi_I)$ ), which obey the following equations of motion:

$$\ddot{\phi}_R + 3H\dot{\phi}_R + m_R^2\phi_R + \lambda_\Phi(\phi_R^2 + \phi_I^2)\phi_R = 0, \quad (2)$$

$$\ddot{\phi}_I + 3H\dot{\phi}_I + m_I^2\phi_I + \lambda_\Phi(\phi_R^2 + \phi_I^2)\phi_I = 0, \quad (3)$$

where  $m_{R,I}^2 = m_\Phi^2 \mp 2A$ . The Hubble expansion rate in a RD Universe is  $H \propto t^{1/2}$ . The overdots denote derivatives with respect to cosmic time  $t$ . We see that the two components have different masses in the presence of  $A \neq 0$ , and thus, the trajectory in the  $\phi_R$ - $\phi_I$  plane is expected to resemble a shrinking ellipse instead of a straight line, even for vanishing initial velocities.

The background field evolution, neglecting the symmetry-breaking term ( $A \ll m_\Phi^2$ ), is initially dominated by the  $|\Phi|^4$  term when the amplitude scales as  $\phi \propto 1/a$ . When the amplitude drops below  $|\Phi_*| = m_\Phi/\sqrt{\lambda_\Phi}$  at  $t = t_*$ , the  $|\Phi|^2$  term dominates the oscillation and the fields evolve approximately as  $\phi_{R,I} \sim a^{-3/2} \cos(m_{R,I}t + c_{R,I})$  (see Section C of the Supplemental Material for details). The  $\Phi$ - $\Phi^\dagger$  asymmetry, which will be transferred later to the baryon (or lepton) number, is  $n_\Phi(t) = i(\Phi^\dagger\dot{\Phi} - \dot{\Phi}^\dagger\Phi) = \dot{\phi}_R\phi_I - \phi_R\dot{\phi}_I$ .  $n_\Phi$  directly corresponds to  $n_B$  or  $n_L$  in the absence of significant washout (see discussion later). Using the above approximations for  $\phi_{R,I}$  and including the terms  $\Gamma_\Phi\dot{\phi}_{R,I}$  to model the decay of  $\Phi$  to SM states, we can write the co-moving baryon asymmetry generated during the time  $t > t_*$  as [54–57]:

$$\left(\frac{a(t)}{a_{\text{in}}}\right)^3 n_B(t) \simeq 4A\phi_{R,\text{in}}\phi_{I,\text{in}} \left(\frac{\phi_{\text{in}}}{\phi_*}\right) \times \int_{t_*}^t dt' \cos(m_R(t' - t_*)) \sin(m_I(t' - t_*)) e^{-\Gamma_\Phi(t' - t_*)}, \quad (4)$$

where the exponential factor accounts for the decrease in  $\Phi$  amplitude due to its decay to SM particles with a constant decay rate  $\Gamma_\Phi$ , enabling the asymmetry transfer to the SM baryons. The specific form of  $\Gamma_\Phi$  depends on the decay channels, which we will elaborate on later. Evaluating the above integral for  $t \rightarrow \infty$  and factoring in the expansion during the RD Universe, we express  $n_B/s$  as

$$\frac{n_B}{s} = \begin{cases} \left(\frac{4\alpha^3}{\lambda_\Phi k_{Td}^6}\right)^{1/4} \epsilon_\Phi \frac{m_\Phi M_{\text{Pl}}}{T_d^2} \sin(2\theta); & \gamma_\Phi \gg 2\epsilon_\Phi \\ \left(\frac{\alpha^3 k_{Td}^2}{64\lambda_\Phi}\right)^{1/4} \frac{1}{\epsilon_\Phi} \frac{T_d^2}{m_\Phi M_{\text{Pl}}} \sin(2\theta); & \gamma_\Phi \ll 2\epsilon_\Phi \end{cases} \quad (5)$$

where  $M_{\text{Pl}} \simeq 2.4 \times 10^{18}$  GeV is the reduced Planck mass, and we define the dimensionless quantities:  $\epsilon_\Phi = A/m_\Phi^2$ ,  $\gamma_\phi = \Gamma_\Phi/m_\Phi$  and  $k_{T_d} = \sqrt{\pi^2 g(T_d)/90}$ .  $T_d$  is the temperature of the Universe when the  $\Phi$  decay is completed at  $H(T_d) = \Gamma_\Phi$ ,  $\alpha$  is the initial fraction of energy density in the spectator sector  $\Phi$  relative to the total energy density, and  $\theta = \theta_{\text{in}}$  is defined earlier. In case the asymmetry is first transferred to SM leptons, a redistribution factor of 28/79 due to the EW sphaleron would be added in the RHS of Eq. (5).

Eq. (5) is derived assuming that the asymmetry is generated when the potential is dominated by the  $|\Phi|^2$  term; thus, we require that the background dynamics prior to  $t_*$ , defined as when  $|\Phi(t_*)| = m_\Phi/\sqrt{\lambda_\Phi}$ , is not affected by the  $A$  term. The corresponding condition on  $A$  can be estimated as follows: The only term in the potential that involves the angular degree of freedom is the symmetry-breaking term  $2A|\Phi(t)|^2 \cos 2\theta(t) \subset V(|\Phi|, \theta)$ , indicating an upper bound on the effective mass along the angular direction:  $|m_\theta^2| \leq 2A$ . The angular degree of freedom is frozen at  $\theta_{\text{in}}$  for  $t < t_*$ , if  $|m_\theta^2| < H^2(t_*)$  [56], which translates to  $\epsilon_\Phi \equiv A/m_\Phi^2 < (\mu^2/16\alpha) (\phi_{\text{in}}^2/M_{\text{Pl}}^2)$ , where  $\mu^2 \equiv m_\Phi^2/(\lambda_\Phi \phi_{\text{in}}^2)$ , and  $\alpha$  is defined below Eq. 5. As we see in the next section, typically  $\phi_{\text{in}} \simeq M_{\text{Pl}}$  and  $\mu^2 \lesssim 10^{-5}$  are required for detectable GW signals. With larger  $A$ , motion along the angular direction is non-negligible, and  $\theta(t)$  would have already evolved towards its minimum before  $t = t_*$ , thus reducing  $\sin \theta$  and suppressing the asymmetry (see Eq. (5)). For our benchmark examples, the chosen  $A$  values satisfy this self-consistency condition.

We now present some numerical examples of the asymmetry. For  $\epsilon_\Phi = 10^{-20}$  the observed  $n_B/s \sim 10^{-10}$  can be realized with  $T_d \sim 2.5 \times 10^7$  GeV when  $m_\Phi = 10$  GeV. As we will discuss, transfer of the asymmetry to the baryon sector may involve significant washout (model-dependent), requiring a larger initial  $\Phi$  asymmetry to compensate. Therefore we also consider the parameter points that lead to  $n_\Phi/s \gg 10^{-10}$ , for example, with the same  $\epsilon_\Phi$ , but  $T_d \sim 1$  GeV, one obtains  $n_\Phi/s \sim 4 \times 10^{-5}$ . A more detailed parameter scan is given in Section C of the Supplemental Material and Fig. S1, demonstrating the possibility of producing a large initial asymmetry to compensate for potential (model-dependent) washout effects.

## II. Transfer to SM baryon asymmetry.

The asymmetry in the  $\Phi$  field generated during its oscillation needs to eventually be transferred to the SM baryon asymmetry via its subsequent decay to baryons or leptons (further assisted by electroweak sphalerons in the latter case). This can generally be realized by a B- or L-violating coupling involving  $\Phi$  in terms of effective higher dimensional operators, such as  $\Phi QQQ/\Lambda^3$  [6],  $\Phi UDDUDD/\Lambda^6$  and  $\Phi LLELLE/\Lambda^6$ . Whether the re-

lated constraints, for instance, from  $n - \bar{n}$  oscillation, can be satisfied depends on the specifics of the UV completion, including flavor structure in the couplings. As a proof of principle, in the following, we outline examples of renormalizable UV complete models realizing the  $\Phi$  to baryon asymmetry transfer and summarize the conditions on viable model parameters. Further details of the analysis are given in Section D of the Supplemental Material. The core results of this work are independent of the details of the asymmetry transfer mechanism.

(A)  $\Phi$  decay to leptons (*leptogenesis*).

A simple renormalizable model involves:

$$\mathcal{L} \supset y_N {}_i \Phi \bar{N}_i^C N_i + g_\nu {}_{ij} \bar{N}_i H L_j + \text{h.c.}, \quad (6)$$

where  $N_i$ 's are right-handed (RH) Majorana neutrinos (with  $i = 1, 2, 3$  as a typical choice),  $H$  is SM Higgs,  $L_j$  are SM lepton doublets. This model potentially relates to neutrino mass generation, which nevertheless is not imposed as a requirement here. We consider the simple scenario where  $\Phi$  decays to  $NN$ , then  $N$  transfers the asymmetry to SM leptons via freeze-out or freeze-in processes enabled by the  $NHL$  coupling, as considered in the literature of leptogenesis [58–63] [64].

(B)  $\Phi$  decay to baryons (*direct baryogenesis*)

A simple renormalizable model, in this case, includes:

$$\mathcal{L} \supset y_\chi \Phi \chi \chi + g_i \chi \bar{u}_i \varphi + \lambda_{ij} \varphi d_i d_j + \text{h.c.}, \quad (7)$$

where  $\chi$  is a singlet Majorana fermion,  $\varphi$  is an up-type diquark scalar, and the flavor indices  $i, j = 1, 2, 3$  in down-type quark combination  $d_i d_j$  should be antisymmetric. In the viable parameter region, the decay proceeds with  $\Phi \rightarrow \chi\chi$ , followed by  $\chi \rightarrow udd$ .

Both models are subject to cosmological conditions which impose lower limits on  $m_\Phi$  and  $m_\chi$  or  $m_N$ . For  $\Phi$  to decay to baryons (before BBN), it is subject to kinematic conditions:  $m_\Phi \gtrsim 2$  GeV, and  $m_\chi \gtrsim 1$  GeV. For  $\Phi$  asymmetry to be transferred to the SM leptons via  $N$  before the EW phase transition,  $m_\Phi > 2m_N \gtrsim O(0.1)$  GeV [59]. In addition, for both models, the potential asymmetry washout effects should be either suppressed or can be compensated by a larger initial  $\Phi$  asymmetry produced during its oscillation (which has been shown viable in the last section). Furthermore, relevant laboratory experiments at energy and intensity frontiers searching for B-violation, color-charged new particles, sterile neutrinos, etc., may provide additional constraints on model parameters. In Section D of the Supplemental Material, we elaborate on relevant constraints and demonstrate examples of viable parameter regions. On the other hand, as we will see in our GW results, an upper limit in mass of  $m_\Phi \lesssim O(10)$  GeV corresponds to the currently detectable GW peak frequency range, which is below  $\sim O(100)$  Hz.

This, combined with the aforementioned cosmological lower limit of  $m_\Phi \gtrsim O(0.1 - 1)$  GeV, demonstrates that intriguingly the parameter range of our interest points to new physics at the energy scale of  $O(0.1 - 10)$  GeV, indicating a new potential complementarity between GW detection and laboratory searches across particle physics frontiers.

**Parametric Resonance and GW Signals.** We have seen that the generation of the baryon asymmetry is determined by the classical motion of  $\Phi$  as an averaged background field. In addition to this classical motion of  $\Phi$ , we must consider the corresponding fluctuations around it, which leads to parametric resonance that may source GWs. We proceed by decomposing  $\phi_{R,I} = \bar{\phi}_{R,I}(t) + \delta\phi_{R,I}(x, t)$ , where  $\bar{\phi}_{R,I}$  describe the classical background motion and  $\delta\phi_{R,I}(x, t)$  correspond to the fluctuations, which have a quantum origin. The evolution of background fields  $\bar{\phi}_{R,I}$  follows Eqs. (2), (3), whereas we expand the fluctuations in Fourier modes as

$$\delta\phi_R(x, t) = \int \frac{d^3k}{(2\pi)^3} \left[ a_{R,k} e^{i\vec{k}\cdot\vec{x}} \delta\phi_{R,k}(t) + h.c. \right] \quad (8)$$

and similarly for  $\delta\phi_I(x, t)$ .

As the background fields oscillate around the minimum of the potential, the fluctuations in momentum-space evolve according to

$$\begin{aligned} & \delta\ddot{\phi}_{R,I} + 3H\delta\dot{\phi}_{R,I} + m_{R,I}^2\delta\phi_{R,I} + \frac{k^2}{a^2}\delta\phi_{R,I} \\ & + \lambda_\phi(3\bar{\phi}_{R,I}^2 + \bar{\phi}_{I,R}^2)\delta\phi_{R,I} + 2\bar{\phi}_I\bar{\phi}_R\delta\phi_{I,R} = 0 \end{aligned} \quad (9)$$

We thus see that, in general, the equations for  $\delta\phi_{R,I}$  are coupled. We first consider the representative limit of  $A = 0$ , where  $m_R = m_I = m_\Phi$  and the background field trajectory is simply a straight line through the origin (for vanishing initial velocities, as is the case here).

In this case, we can rotate our field basis and define fields in the radial direction (along the background motion)  $\phi_{\parallel}$  and perpendicular to it (orthogonal direction) as  $\phi_{\perp}$ . By construction,  $\dot{\bar{\phi}}_{\perp} = 0$ , and the fluctuation equations for  $\phi_{\parallel}$  and  $\phi_{\perp}$  decouple, namely,

$$\delta\ddot{\phi}_{\parallel,\perp} + 3H\delta\dot{\phi}_{\parallel,\perp} + \left( \frac{k^2}{a^2} + m_\Phi^2 + q_{\parallel,\perp}\lambda_\Phi\bar{\phi}_{\parallel,\perp}^2 \right) \delta\phi_{\parallel,\perp} = 0 \quad (10)$$

where  $q_{\parallel,\perp} = \{3, 1\}$ . As the background field oscillates quasi-periodically around the origin, fluctuations can be exponentially amplified for certain ranges of wavenumbers. Through the exponential amplification, the occupation number of these modes grows rapidly, and they can thus be treated classically [65, 66]. This phenomenon is referred to as ‘‘preheating’’ [67] in the context of primordial particle production following inflation, while it also

can occur for oscillating spectator scalar fields in general (see, for instance, our related work [48]).

To quantify parametric resonance, we start by defining a dimensionless field amplitude  $\tilde{\phi} = \phi/\phi_{\text{in}}$  and a corresponding conformal scaling for time as  $d\eta = \sqrt{\lambda_\Phi}\phi_{\text{in}}dt/a$  with  $\phi_{\text{in}}$  being the initial amplitude of the scalar field  $\phi_{\text{in}} = |\Phi|_{\text{in}}$ . The dimensionless fluctuation equation becomes (derivatives are over  $\eta$ )

$$\delta\phi''_{\parallel,\perp} + 2\tilde{H}\delta\phi'_{\parallel,\perp} + \left( \tilde{k}^2 + a^2\mu^2 + q_{\parallel,\perp}a^2\tilde{\phi}^2 \right) \delta\phi_{\parallel,\perp} = 0 \quad (11)$$

where  $\tilde{k}^2 = k^2/\lambda_\Phi\phi_{\text{in}}^2$  and  $\tilde{\phi} = \bar{\phi}/\phi_{\text{in}}$ .

There are two essential resonance parameters:  $\mu^2 = \frac{m_\Phi^2}{\lambda_\Phi\phi_{\text{in}}^2}$  and  $q_{\parallel,\perp}$ . As shown in [67], a large  $\mu^2$  can suppress the resonance and determine if the system displays *stable resonance*, *stochastic resonance*, or *no decay*. We choose to focus on  $\mu \leq 10^{-5}$ , such that the system is always in a stable resonance regime. For such small  $\mu^2$ , the system is similar to the well-studied case of a quartic field during preheating, whereas  $q_{\parallel,\perp}$  is fixed in our case due to the rotational symmetry of the potential for  $A = 0$ . Section E of the Supplemental Material discusses in detail the effect of  $q_{\parallel,\perp}$  on the growth of  $\delta\phi_{\parallel,\perp}$  and shows that for sufficiently small values of the asymmetry parameter  $A \lesssim 0.005m_\Phi^2$ , the parametric resonance dynamics is indistinguishable from the case  $A = 0$ , and thus the GWs amplitude remains insensitive to the value of  $A$ . Fortunately, the parameter range of  $A$  that produces sufficient baryon asymmetry, as considered in our benchmarks, is well within this regime. On a technical note, we use the parametrization or real and imaginary components of  $\Phi$  ( $\phi_R, \phi_I$ ) when computing the baryon asymmetry, whereas we are using the radial direction and its orthogonal ( $\phi_{\parallel}, \phi_{\perp}$ ) when computing parametric resonance for  $A \ll m_\Phi^2$ . This is due to the fact that the baryon asymmetry scales with  $A$  and thus the difference between the  $\phi_I$  and  $\phi_R$  directions is important, whereas the parametric resonance and GW production is blind to  $A \ll m_\Phi^2$  and thus the radial coordinates are naturally used. Interesting deviations from the  $A = 0$  limit are discussed in Section E of the Supplemental Material. For  $A \gtrsim 0.05m_\Phi^2$  the GW spectrum starts to be sensitive to the exact value of  $A$  as well as the initial angle  $\theta_{\text{in}}$ . This provides intriguing possibilities for distinguishing between these parameters by dedicated analysis of the GW spectral shape.

The growth of fluctuations and their back-reaction break the homogeneous oscillation of  $\Phi$ , leading to the inhomogeneous structure of scalar fields with an effective anisotropic stress tensor  $\Pi_{ij}^{TT} = \nabla_i\phi^a\nabla_j\phi^a$  (where the repeated index ‘ $a$ ’ indicates the number of the scalar components and a summation is implied). These time-dependent field inhomogeneities source (sub-

Hubble) gravitational waves whose frequency depends on the characteristic energy scale involved  $H_c$ . The peak amplitude and frequency of GW spectra generated from sources peaked at some characteristic scale  $k_c$  in momentum-space can be estimated as [68]

$$f_{\text{GW}}^{\text{peak}} = 2.7 \times 10^{10} \sqrt{\frac{H_c}{M_{\text{P}}}} \frac{k_c}{H_c} \text{ Hz}, \quad (12)$$

$$\Omega_{\text{GW}}^{\text{peak}} = 2.3 \times 10^{-4} \alpha^2 \beta w \left(\frac{k_c}{\sigma}\right) \left(\frac{H_c}{k_c}\right)^2. \quad (13)$$

where  $\alpha$  is a measure of the fraction of the energy in the GW source here the scalar field inhomogeneities and this  $\alpha$  coincides with the  $\alpha$  we defined below Eq. 5 relative to the total energy density of the Universe, and  $\beta$  describes the degree of anisotropy of the source which must be determined from simulations. In typical scenarios  $\beta = \mathcal{O}(0.01 - 0.1)$ . The equation of the state of the Universe at the time of the production of GWs for a radiation-dominated Universe is  $w = 1/3$  and  $\sigma$  is the width of the source in momentum-space, which can be taken as  $\sigma \sim k_c$  for peaked sources (see Ref. [68] for the derivation and e.g. Refs. [48, 69] for further applications of Eqs (12) and (13)).

The dynamics of the generated GWs are governed by the linearized equation for the transverse-traceless tensor perturbation sourced by the above anisotropic stress

$$\ddot{h}_{ij} + 3H\dot{h}_{ij} - \frac{\nabla^2 h_{ij}}{a^2} = \frac{2}{a^2 M_{\text{P}}^2} \Pi_{ij}^{TT}, \quad (14)$$

The quantity of interest is the energy density power spectrum of the GWs normalized by the critical energy density of the Universe today. For GWs produced in a radiation-dominated era, the spectrum of the energy density of GWs (per logarithmic momentum interval) observable today is [13, 48, 70–74]:

$$\begin{aligned} \Omega_{\text{GW},0} h^2 &= \left. \frac{h^2}{\rho_{\text{crit}}} \frac{d\rho_{\text{GW}}}{d \ln k} \right|_{t=t_0} = \left. \frac{h^2}{\rho_{\text{crit}}} \frac{d\rho_{\text{GW}}}{d \ln k} \right|_{t=t_e} \frac{a_e^4 \rho_e}{a_0^4 \rho_{\text{crit},0}} \\ &= \Omega_{\text{rad},0} h^2 \Omega_{\text{GW},e} \left(\frac{g_*}{g_0}\right)^{-1/3}, \end{aligned} \quad (15)$$

where the critical density of the Universe is  $\rho_{\text{crit}} = 3M_{\text{P}}^2 H^2$  and  $\Omega_{\text{rad},0} h^2 = h^2 \rho_{\text{rad},0} / \rho_{\text{crit}} = 4.3 \times 10^{-5}$ . In particular, we employ the publicly available code Cosmolattice [75, 76] in a three-dimensional lattice, in order to numerically solve the metric perturbation equations in Eq. (14) along with the equations for the scalar system in an expanding universe.

The benchmark examples of observed spectra today from our model simulation are shown in Fig 1. For the initially  $\Phi^4$  dominant system, as in our case, the field starts

rolling/oscillating when  $H \sim \sqrt{\lambda_\Phi} \phi_{\text{in}}$ . This combination of  $\sqrt{\lambda_\Phi} \phi_{\text{in}}$  also determines the frequency of the observed GWs, according to Eq. 12. We consider the RD universe with the scalar field system contributing to a fraction of the total energy  $\alpha$  and  $\alpha = 0.3$  is assumed in Fig 1. According to Eq. 13,  $\Omega_{\text{GW}}^{\text{peak}} \propto \alpha^2 \propto \phi_{\text{in}}^8$ , and we found that a sizable  $\alpha \sim \mathcal{O}(0.1)$  which optimizes GW amplitude requires  $\phi_{\text{in}} \sim M_{\text{P}}$ . As we have seen from the discussion on the resonance structure of the model, the parameters  $\mu_{\pm}$  (or simply  $\mu$  when  $A = 0$ ) determine the nature and efficiency of resonance [67]. We take  $\mu = 10^{-5}$  as an example for stable resonance, which fixes  $\lambda_\Phi \phi_{\text{in}}^2$ . with the optimal choice of  $\phi_{\text{in}} \sim M_{\text{P}1}$ , we find  $\lambda_\Phi \sim 10^{-30}$  for the mass range of interest. As discussed earlier,  $m_\Phi \gtrsim \mathcal{O}(0.1)$  GeV is required for  $\Phi$  to successfully transfer the asymmetry to SM baryons. Interestingly, in the viable range of  $m_\Phi \sim \mathcal{O}(0.1) - \mathcal{O}(10)$  GeV, the resulting peak GW frequency lies well within the range of ET/CE and with sufficient amplitudes, making signal detection promising for the near future. A higher range of  $m_\Phi$  is compatible with baryogenesis but requires futuristic higher frequency GW detectors [77] to capture the peak frequency range of the signal. Due to the finite box size and lattice spacing, low-frequency modes well off the peak cannot be resolved in our simulation, which is a common issue in the lattice simulation literature [13]. Therefore, to extend the spectral prediction to lower frequencies, we apply the standard assumption that at low wave numbers, the GW spectrum grows as  $k^3$ , as derived from causality arguments [13, 78, 79]. This is shown in dashed lines in Fig. 1. Depending on  $m_\Phi$ , the low- $k$  tail may be detectable by DECIGO and BBO, providing the prospect for a correlated detection across multiple frequency bands, probing the peak and tail of the spectrum simultaneously.

Finally, note that since  $\Phi$  is coupled to SM fermions in order to transfer the asymmetry to baryons, the effect of parametric excitation of these fermionic states should be evaluated. Nevertheless, in the context of preheating, it was found that during scalar field oscillations, the energy transfer to bosons is typically faster and larger than to fermions due to Pauli blocking [80–84]. Therefore, we expect our resonance analysis to remain robust in the presence of fermion couplings.

**Conclusion and Outlook.** In this *Letter*, we first demonstrate that the Affleck-Dine mechanism for baryogenesis can be realized by a complex light scalar field  $\Phi$  with a mass  $m_\Phi$  well below the electroweak scale without invoking supersymmetry. In particular, we use a convex, renormalizable, polynomial potential (which does not lead to the formation of Q-balls generally present in SUSY AD models). Such a scalar field acts as a spectator field during inflation while acquiring a large field value at the end of inflation. The subsequent rolling down

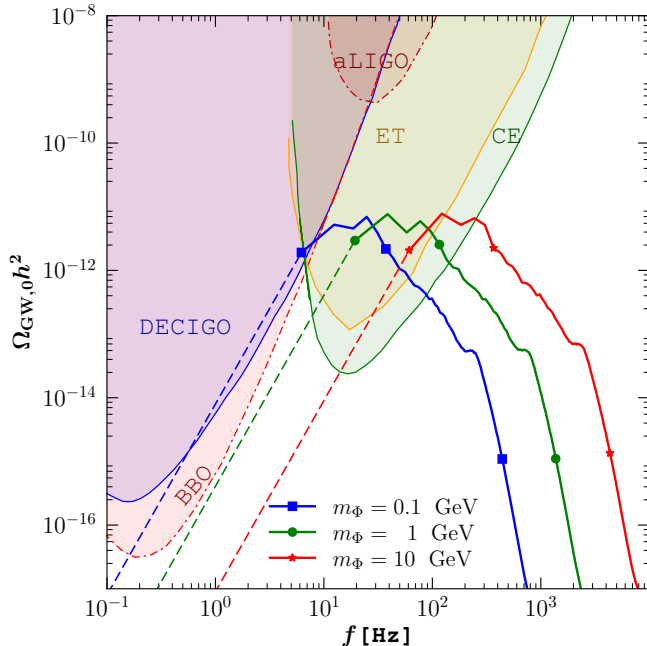


FIG. 1. We show the GW spectrum originating from the AD model considered here for three benchmark masses of  $\Phi$ . The potential parameters  $\lambda_\Phi = 10^{-30}$ ,  $A = 0$  are chosen to ensure efficient parametric resonance (see main text for details). The fraction of initial scalar field energy density over the total energy density of the Universe is  $\alpha = 30\%$ . The dashed lines at lower frequencies are extrapolated according to the causal super-horizon  $k^3$  scaling.

and oscillation of the scalar field occur long after inflation, during the radiation-dominated era, triggering the generation of baryon asymmetry. Parametric resonance and fragmentation generally arise during the oscillation of the scalar field, naturally leading to GW production. We demonstrate that the theory may lead to successful baryogenesis while sourcing detectable GW signals with a peak frequency of  $\mathcal{O}(10\text{-}100)$  Hz, within reach of experiments such as ET and CE. Furthermore, the characteristic new physics scale, characterized by  $m_\Phi$ , intriguingly lies in the range of  $\mathcal{O}(0.1\text{-}10)$  GeV, while the transfer of the  $\Phi$  asymmetry to the SM B- or L-asymmetry requires interactions between the new physics sector and the SM states. Hence, from this well-motivated scenario, a new, natural complementarity arises between SGWB detection and laboratory searches for new particle physics across the energy, intensity, and neutrino frontiers. The specifics of the complementary laboratory signal depend on the details of the asymmetry transfer mechanism. Examples include: searches for  $\mathcal{O}(0.1\text{-}10)$  GeV mass sterile neutrino with DUNE, SHiP, FASER, etc. and exotic multi-jet signals at the LHC (see Section D of the Supplemen-

tal Material). This work thus sheds new light on probing early Universe baryogenesis through its GW imprint, potentially complemented by associated laboratory probes, while presenting a well-motivated new physics source for SGWB.

**Acknowledgements.** We thank Brian Shuve for helpful discussions. YC is supported by the US Department of Energy under award number DE-SC0008541. AG is supported by "Excellence Initiative - Research University (2020-2026)" IDUB grant. PS is supported by Grant-in-Aid for Scientific Research (B) under Contract No. 23K25873 (23H01177). Numerical computation in this work was carried out at the Yukawa Institute Computer Facility. EIS acknowledges support by the U.S. Department of Energy, Office of Science, Office of High Energy Physics program under Award Number DE-SC0022021.

\* yanou.cui@ucr.edu

† anish.ghoshal@fuw.edu.pl

‡ pankaj@post.kek.jp

§ evangelos.sfakianakis@austin.utexas.edu

- [1] N. Aghanim *et al.* (Planck), *Astron. Astrophys.* **641**, A6 (2020), [Erratum: *Astron. Astrophys.* 652, C4 (2021)], arXiv:1807.06209 [astro-ph.CO].
- [2] I. Affleck and M. Dine, *Nucl. Phys. B* **249**, 361 (1985).
- [3] M. Dine, L. Randall, and S. D. Thomas, *Nucl. Phys. B* **458**, 291 (1996), arXiv:hep-ph/9507453.
- [4] M. Dine and A. Kusenko, *Rev. Mod. Phys.* **76**, 1 (2003), arXiv:hep-ph/0303065.
- [5] K. Enqvist and A. Mazumdar, *Phys. Rept.* **380**, 99 (2003), arXiv:hep-ph/0209244.
- [6] R. Allahverdi and A. Mazumdar, *New J. Phys.* **14**, 125013 (2012).
- [7] M. P. Hertzberg and J. Karouby, *Phys. Rev. D* **89**, 063523 (2014), arXiv:1309.0010 [hep-ph].
- [8] J. M. Cline, M. Puel, and T. Toma, *Phys. Rev. D* **101**, 043014 (2020), arXiv:1909.12300 [hep-ph].
- [9] N. Kitajima, J. Soda, and Y. Urakawa, *JCAP* **10**, 008 (2018), arXiv:1807.07037 [astro-ph.CO].
- [10] D. G. Figueroa and F. Torrenti, *JCAP* **10**, 057 (2017), arXiv:1707.04533 [astro-ph.CO].
- [11] K. D. Lozanov and M. A. Amin, *Phys. Rev. D* **99**, 123504 (2019), arXiv:1902.06736 [astro-ph.CO].
- [12] T. Hiramatsu, E. I. Sfakianakis, and M. Yamaguchi, *JHEP* **03**, 021 (2021), arXiv:2011.12201 [hep-ph].
- [13] R. Easther, J. T. Giblin, Jr., and E. A. Lim, *Phys. Rev. Lett.* **99**, 221301 (2007), arXiv:astro-ph/0612294.
- [14] R. Friedberg, T. D. Lee, and A. Sirlin, *Phys. Rev. D* **13**, 2739 (1976).
- [15] S. R. Coleman, *Nucl. Phys. B* **262**, 263 (1985), [Addendum: *Nucl. Phys. B* 269, 744 (1986)].
- [16] A. Kusenko, *Phys. Lett. B* **404**, 285 (1997), arXiv:hep-th/9704073.

- [17] A. Kusenko and M. E. Shaposhnikov, *Phys. Lett. B* **418**, 46 (1998), arXiv:hep-ph/9709492.
- [18] A. Kusenko and A. Mazumdar, *Phys. Rev. Lett.* **101**, 211301 (2008), arXiv:0807.4554 [astro-ph].
- [19] A. Kusenko, A. Mazumdar, and T. Multamaki, *Phys. Rev. D* **79**, 124034 (2009), arXiv:0902.2197 [astro-ph.CO].
- [20] S.-Y. Zhou, *JCAP* **06**, 033 (2015), arXiv:1501.01217 [astro-ph.CO].
- [21] In SUSY-based AD models, producing detectable strength of GWs can typically lead to  $\eta_B \gg 10^{-10}$  [18, 19]. Therefore, [18, 19] considered GWs from AD flat-direction fields with  $B-L=0$ , which is not relevant for baryogenesis. Furthermore, recent lattice simulations revealed that the typical frequency of the GWs generated from SUSY AD models is higher than the currently detectable range [20]. Finally, the term  $|\Phi|^2 \log(|\Phi|/M_{\text{Pl}})$  in the potential considered in [18–20] exhibits a pathology at  $\Phi=0$  (the impact of which on their GW results warrants re-examination), a pathology absent in our polynomial potential.
- [22] G. White, L. Pearce, D. Vagie, and A. Kusenko, *Phys. Rev. Lett.* **127**, 181601 (2021), arXiv:2105.11655 [hep-ph].
- [23] K. Kohri and T. Terada, *Phys. Rev. D* **97**, 123532 (2018), arXiv:1804.08577 [gr-qc].
- [24] B. P. Abbott *et al.* (LIGO Scientific), *Class. Quant. Grav.* **34**, 044001 (2017), arXiv:1607.08697 [astro-ph.IM].
- [25] S. Hild, S. Chelkowski, and A. Freise, (2008), arXiv:0810.0604 [gr-qc].
- [26] S. Kawamura *et al.*, *PTEP* **2021**, 05A105 (2021), arXiv:2006.13545 [gr-qc].
- [27] G. M. Harry, P. Fritschel, D. A. Shaddock, W. Folkner, and E. S. Phinney, *Class. Quant. Grav.* **23**, 4887 (2006), [Erratum: *Class. Quant. Grav.* **23**, 7361 (2006)].
- [28] B. P. Abbott *et al.* (LIGO Scientific, Virgo), *Phys. Rev. Lett.* **116**, 061102 (2016), arXiv:1602.03837 [gr-qc].
- [29] B. P. Abbott *et al.* (LIGO Scientific, Virgo), *Phys. Rev. Lett.* **116**, 241103 (2016), arXiv:1606.04855 [gr-qc].
- [30] F. Acernese *et al.* (VIRGO), *Class. Quant. Grav.* **32**, 024001 (2015), arXiv:1408.3978 [gr-qc].
- [31] C. L. Carilli and S. Rawlings, *New Astron. Rev.* **48**, 979 (2004), arXiv:astro-ph/0409274.
- [32] A. Weltman *et al.*, *Publ. Astron. Soc. Austral.* **37**, e002 (2020), arXiv:1810.02680 [astro-ph.CO].
- [33] L. Lentati *et al.* (EPTA), *Mon. Not. Roy. Astron. Soc.* **453**, 2576 (2015), arXiv:1504.03692 [astro-ph.CO].
- [34] S. Babak *et al.* (EPTA), *Mon. Not. Roy. Astron. Soc.* **455**, 1665 (2016), arXiv:1509.02165 [astro-ph.CO].
- [35] G. Agazie *et al.* (NANOGrav), *Astrophys. J. Lett.* **951**, L8 (2023), arXiv:2306.16213 [astro-ph.HE].
- [36] A. Afzal *et al.* (NANOGrav), *Astrophys. J. Lett.* **951**, L11 (2023), arXiv:2306.16219 [astro-ph.HE].
- [37] J. Antoniadis *et al.* (EPTA), *Astron. Astrophys.* **678**, A48 (2023), arXiv:2306.16224 [astro-ph.HE].
- [38] J. Antoniadis *et al.* (EPTA), *Astron. Astrophys.* **678**, A50 (2023), arXiv:2306.16214 [astro-ph.HE].
- [39] G. Aad *et al.* (ATLAS), *JHEP* **02**, 143 (2021), arXiv:2010.14293 [hep-ex].
- [40] M. Aaboud *et al.* (ATLAS), *Phys. Lett. B* **785**, 136 (2018), arXiv:1804.03568 [hep-ex].
- [41] P. D. Bolton, F. F. Deppisch, and P. S. Bhupal Dev, *JHEP* **03**, 170 (2020), arXiv:1912.03058 [hep-ph].
- [42] A. Ariga *et al.* (FASER), *Phys. Rev. D* **99**, 095011 (2019), arXiv:1811.12522 [hep-ph].
- [43] P. Ballett, T. Boschi, and S. Pascoli, *JHEP* **03**, 111 (2020), arXiv:1905.00284 [hep-ph].
- [44] K. Abe *et al.* (T2K), *Phys. Rev. D* **100**, 052006 (2019), arXiv:1902.07598 [hep-ex].
- [45] M. Drewes, J. Hajer, J. Klaric, and G. Lanfranchi, *JHEP* **07**, 105 (2018), arXiv:1801.04207 [hep-ph].
- [46] R. Barouki, G. Marocco, and S. Sarkar, *SciPost Phys.* **13**, 118 (2022), arXiv:2208.00416 [hep-ph].
- [47] A. A. Starobinsky and J. Yokoyama, *Phys. Rev. D* **50**, 6357 (1994), arXiv:astro-ph/9407016.
- [48] Y. Cui, P. Saha, and E. I. Sfakianakis, *Phys. Rev. Lett.* **133**, 021004 (2024), arXiv:2310.13060 [hep-ph].
- [49] R. J. Hardwick, V. Vennin, C. T. Byrnes, J. Torrado, and D. Wands, *JCAP* **10**, 018 (2017), arXiv:1701.06473 [astro-ph.CO].
- [50] T. Markkanen, A. Rajantie, and T. Tenkanen, *Phys. Rev. D* **98**, 123532 (2018), arXiv:1811.02586 [astro-ph.CO].
- [51] T. Markkanen, A. Rajantie, S. Stopyra, and T. Tenkanen, *JCAP* **08**, 001 (2019), arXiv:1904.11917 [gr-qc].
- [52] Other mechanisms can be invoked to drive the  $\Phi$  field to large values during inflation, like a non-minimal coupling to gravity or a direct coupling to the inflaton. Our results for the GWs and baryon asymmetry do not depend on the origin of  $\Phi_{\text{in}}$ .
- [53] Since we consider small  $U(1)$  symmetry-breaking terms, the angular field will always be light when the radial field is light.
- [54] V. A. Rubakov and D. S. Gorbunov, *Introduction to the Theory of the Early Universe: Hot big bang theory* (World Scientific, Singapore, 2017).
- [55] A. Lloyd-Stubbs and J. McDonald, *Phys. Rev. D* **103**, 123514 (2021), arXiv:2008.04339 [hep-ph].
- [56] K. Lloyd-Stubbs and J. McDonald, *Phys. Rev. D* **107**, 103511 (2023), arXiv:2212.09454 [hep-ph].
- [57] R. N. Mohapatra and N. Okada, *Phys. Rev. D* **104**, 055030 (2021), arXiv:2107.01514 [hep-ph].
- [58] E. K. Akhmedov, V. A. Rubakov, and A. Y. Smirnov, *Phys. Rev. Lett.* **81**, 1359 (1998), arXiv:hep-ph/9803255.
- [59] J. Klarić, M. Shaposhnikov, and I. Timiryasov, *Phys. Rev. Lett.* **127**, 111802 (2021), arXiv:2008.13771 [hep-ph].
- [60] J. Klarić, M. Shaposhnikov, and I. Timiryasov, *Phys. Rev. D* **104**, 055010 (2021), arXiv:2103.16545 [hep-ph].
- [61] Y. Cui, L. Randall, and B. Shuve, *JHEP* **08**, 073 (2011), arXiv:1106.4834 [hep-ph].
- [62] T. Hambye and D. Teresi, *Phys. Rev. Lett.* **117**, 091801 (2016), arXiv:1606.00017 [hep-ph].
- [63] I. Flood, R. Porto, J. Schlesinger, B. Shuve, and M. Thum, *Phys. Rev. D* **105**, 095025 (2022), arXiv:2109.10908 [hep-ph].
- [64] Unlike in leptogenesis, here we do not require additional CP violation or out-of-equilibrium condition in neutrino

- sector to generate the asymmetry, as the asymmetry is already generated in  $\Phi$ .
- [65] D. Polarski and A. A. Starobinsky, Nucl. Phys. B **385**, 623 (1992).
- [66] L. Kofman, A. D. Linde, and A. A. Starobinsky, Phys. Rev. D **56**, 3258 (1997), arXiv:hep-ph/9704452.
- [67] P. B. Greene, L. Kofman, A. D. Linde, and A. A. Starobinsky, Phys. Rev. D **56**, 6175 (1997), arXiv:hep-ph/9705347.
- [68] J. T. Giblin and E. Thrane, Phys. Rev. D **90**, 107502 (2014), arXiv:1410.4779 [gr-qc].
- [69] Y. Cui and E. I. Sfakianakis, Phys. Lett. B **840**, 137825 (2023), arXiv:2112.00762 [hep-ph].
- [70] R. Easther and E. A. Lim, JCAP **04**, 010 (2006), arXiv:astro-ph/0601617.
- [71] R. Easther, J. T. Giblin, and E. A. Lim, Phys. Rev. D **77**, 103519 (2008), arXiv:0712.2991 [astro-ph].
- [72] J. F. Dufaux, A. Bergman, G. N. Felder, L. Kofman, and J.-P. Uzan, Phys. Rev. D **76**, 123517 (2007), arXiv:0707.0875 [astro-ph].
- [73] J. Garcia-Bellido and D. G. Figueroa, Phys. Rev. Lett. **98**, 061302 (2007), arXiv:astro-ph/0701014.
- [74] J. Garcia-Bellido, D. G. Figueroa, and A. Sastre, Phys. Rev. D **77**, 043517 (2008), arXiv:0707.0839 [hep-ph].
- [75] D. G. Figueroa, A. Florio, F. Torrenti, and W. Valkenburg, JCAP **04**, 035 (2021), arXiv:2006.15122 [astro-ph.CO].
- [76] D. G. Figueroa, A. Florio, F. Torrenti, and W. Valkenburg, Comput. Phys. Commun. **283**, 108586 (2023), arXiv:2102.01031 [astro-ph.CO].
- [77] N. Aggarwal *et al.*, Living Rev. Rel. **24**, 4 (2021), arXiv:2011.12414 [gr-qc].
- [78] C. Caprini, R. Durrer, T. Konstandin, and G. Servant, Phys. Rev. D **79**, 083519 (2009), arXiv:0901.1661 [astro-ph.CO].
- [79] A. Hook, G. Marques-Tavares, and D. Racco, JHEP **02**, 117 (2021), arXiv:2010.03568 [hep-ph].
- [80] P. B. Greene and L. Kofman, Phys. Lett. B **448**, 6 (1999), arXiv:hep-ph/9807339.
- [81] G. F. Giudice, M. Peloso, A. Riotto, and I. Tkachev, JHEP **08**, 014 (1999), arXiv:hep-ph/9905242.
- [82] P. B. Greene and L. Kofman, Phys. Rev. D **62**, 123516 (2000), arXiv:hep-ph/0003018.
- [83] L. Sorbo, Nucl. Phys. B Proc. Suppl. **95**, 86 (2001).
- [84] P. Adshead and E. I. Sfakianakis, JCAP **11**, 021 (2015), arXiv:1508.00891 [hep-ph].
- [85] P. Adshead, L. Pearce, J. Shelton, and Z. J. Weiner, Phys. Rev. D **102**, 023526 (2020), arXiv:2002.07201 [hep-ph].
- [86] S. Kasuya, M. Kawasaki, and F. Takahashi, JCAP **10**, 017 (2008), arXiv:0805.4245 [hep-ph].
- [87] M. S. Turner, Phys. Rev. **D28**, 1243 (1983).
- [88] J. A. Harvey and M. S. Turner, Phys. Rev. D **42**, 3344 (1990).
- [89] T. Asaka, H. B. Nielsen, and Y. Takanishi, Nucl. Phys. B **647**, 252 (2002), arXiv:hep-ph/0207023.
- [90] J. Garcia-Bellido, D. Y. Grigoriev, A. Kusenko, and M. E. Shaposhnikov, Phys. Rev. D **60**, 123504 (1999), arXiv:hep-ph/9902449.
- [91] B. Shuve and I. Yavin, Phys. Rev. D **89**, 075014 (2014), arXiv:1401.2459 [hep-ph].
- [92] J. M. Cline, M. Puel, and T. Toma, JHEP **05**, 039 (2020), arXiv:2001.11505 [hep-ph].
- [93] (2022), <https://www.hep.ucl.ac.uk/~pbolton/plots.html>.
- [94] Y. Cui and R. Sundrum, Phys. Rev. D **87**, 116013 (2013), arXiv:1212.2973 [hep-ph].
- [95] S. Karmakar (ATLAS, CMS, LHCb), PoS **LHCP2022**, 073 (2023).
- [96] A. M. Sirunyan *et al.* (CMS), Phys. Rev. D **98**, 112014 (2018), arXiv:1808.03124 [hep-ex].
- [97] A. M. Sirunyan *et al.* (CMS), Phys. Rev. D **104**, 052001 (2021), arXiv:2103.01290 [hep-ex].
- [98] J. M. Arnold, B. Fornal, and M. B. Wise, Phys. Rev. D **87**, 075004 (2013), arXiv:1212.4556 [hep-ph].
- [99] J. L. Goity and M. Sher, Phys. Lett. B **346**, 69 (1995), [Erratum: Phys.Lett.B 385, 500 (1996)], arXiv:hep-ph/9412208.
- [100] R. Barbier *et al.*, Phys. Rept. **420**, 1 (2005), arXiv:hep-ph/0406039.
- [101] C. Brust, A. Katz, S. Lawrence, and R. Sundrum, JHEP **03**, 103 (2012), arXiv:1110.6670 [hep-ph].
- [102] C. Brust, A. Katz, and R. Sundrum, JHEP **08**, 059 (2012), arXiv:1206.2353 [hep-ph].
- [103] R. Franceschini and R. Torre, Eur. Phys. J. C **73**, 2422 (2013), arXiv:1212.3622 [hep-ph].
- [104] T. Zhang, H. Yang, D. Martynov, P. Schmidt, and H. Miao, Phys. Rev. X **13**, 021019 (2023), arXiv:2212.12144 [gr-qc].
- [105] Y. Chen, B. Liu, S. Ai, L. Lan, H. Gao, Y. Yuan, and Z.-H. Zhu, Mon. Not. Roy. Astron. Soc. **527**, 6055 (2023), arXiv:2311.09654 [gr-qc].



# The Origin Symphony: Probing Baryogenesis with Gravitational Waves

## *Supplemental Material*

Yanou Cui, Anish Ghoshal, Pankaj Saha and Evangelos I. Sfakianakis

### A. Inflationary fluctuations and initial conditions

In some versions of the Affleck-Dine mechanism, an extra coupling is introduced in the potential in order to generate a radial minimum at large field values [6]. We argue that this is not necessary for the AD field to acquire a large initial value. It has been known that a light scalar field in de-Sitter space-time acquires quantum fluctuations, eventually leading to an equilibrium distribution [47]. In the case of a quartic real scalar field with  $V = \frac{1}{4}\lambda\phi^4$ , the variance of the equilibrium distribution is  $\langle\phi^2\rangle \sim H^2/\sqrt{\lambda}$ , whereas for a quadratic field  $V = \frac{1}{2}m^2\phi^2$  we arrive at  $\langle\phi^2\rangle \sim H^4/m^2$ . As an example,  $\langle\phi^2\rangle \sim M_{\text{Pl}}^2$  and  $0.1 \text{ GeV} \lesssim m \lesssim 10 \text{ GeV}$  requires an inflationary Hubble scale of at least  $10^{-10}M_{\text{Pl}} \lesssim H \lesssim 10^{-9}M_{\text{Pl}}$  for quadratic fields. If the quartic term dominates during inflation with  $\lambda \sim 10^{-30}$  a Planckian standard deviation requires  $H \sim 10^{-15}M_{\text{Pl}}$  or greater. The variance of the distribution grows as  $\langle\phi^2\rangle = (H^2/4\pi^2)N$  where  $N$  is the  $e$ -folding number. We thus see that an equilibrium distribution with a Planckian standard deviation requires much more than the usual minimum amount of 60  $e$ -folds of inflation. This may be considered as a way to infer whether a prolonged inflationary phase took place in the early universe.

The above discussion (see Ref. [48] for more details) applies to the absolute value of the complex scalar field  $|\phi|$ . The argument will enter its equilibrium distribution much sooner, and the distribution itself will be much simpler: uniform between 0 and  $2\pi$ . The intricacies of multi-dimensional random walks and their applications to de Sitter fluctuations of fields with continuous symmetries (including complex scalars) can be found in Ref. [85]. Finally, a large initial field value  $\phi_{\text{in}}$  could simply result from an ad hoc initial condition. One may argue that the initial condition for the inflaton itself is set ad hoc, although quantum fluctuations can be invoked to explain it. Most importantly, our results are independent of the details of how  $\phi_{\text{in}}$  is realized (the same is true for the inflationary attractor).

### B. Isocurvature perturbations

In our previous work [48], we briefly discussed the possible isocurvature fluctuations from spectator scalar fields during inflation. In the current case, there are two degrees of freedom due to the complex nature of the AD field. If we decompose the complex scalar into a radial and an angular degree of freedom, the radial field will have similar behavior to a real scalar (for slight quantitative differences, see [85]), with isocurvature fluctuations that scale as  $\mathcal{P}_{\mathcal{S}} \sim H_I^2/M_{\text{Pl}}^2$  if we take the initial value of the radial field to be  $\mathcal{O}(M_{\text{Pl}})$  originating solely from de-Sitter fluctuations as described in Section A. We thus see that for reasonable values of the inflationary Hubble scale  $H_I$ , these fluctuations are suppressed. Furthermore, if the AD field decays to SM particles, we can expect the isocurvature perturbation to vanish.

However, the angular degree of freedom, which is responsible for the baryon number, also receives de Sitter fluctuations during inflation. This means that the AD mechanism proceeds differently in different parts of the Universe due to the fluctuations in the initial condition for the angular field. This leads to baryon isocurvature fluctuations, which are more constrained by the measurement of the CMB.

We follow previous computations of isocurvature fluctuations in models of AD baryogenesis, in particular, Ref. [7]; see also [86]. During inflation we can decompose the AD field  $\Phi$  into a radial component  $R$  and an angular component  $\theta$ . We consider a typical value of the radial field  $\bar{R} = \sqrt{\langle R^2 \rangle} \sim M_{\text{Pl}}$  and thus

$$\langle\delta\theta^2\rangle \simeq \frac{1}{4\pi^2} \frac{H_I^2}{\bar{R}^2} \quad (\text{S1})$$

Ref. [7] introduced a multiplicative  $\mathcal{O}(1)$  factor to account for the two-dimensional random walk of a complex scalar (see also Ref. [85]). Since the baryon number is proportional to  $\sin(n\theta)$  the normalized first order fluctuations  $\delta n_b$  follow

$$\frac{\delta n_b}{n_b} = n\delta\theta \cot(\theta) \quad (\text{S2})$$

The corresponding power of the baryon isocurvature temperature fluctuations is

$$\left\langle \left( \frac{\delta T}{T} \right) \right\rangle_{\text{isoc}} \simeq 0.004 \frac{\Omega_b^2}{\Omega_m^2} \frac{n^2 H^2}{\bar{R}^2} \cot^2(n\theta) \quad (\text{S3})$$

We can take  $\cot^2(n\theta) \sim 1$  and  $\Omega_b/\Omega_m \simeq 0.16$ , leading to

$$\left\langle \left( \frac{\delta T}{T} \right) \right\rangle_{\text{isoc}} \simeq 10^{-4} \frac{n^2 H^2}{\bar{R}^2} \quad (\text{S4})$$

Taking a simple model of single-field inflation for simplicity and following again Ref. [7]

$$\left\langle \left( \frac{\delta T}{T} \right) \right\rangle_{\text{adiabatic}} \simeq \frac{1}{20} \frac{H^2}{8\pi^2 M_{\text{Pl}}^2 \epsilon} = \frac{1}{20} \frac{H^2}{8\pi^2 M_{\text{Pl}}^2 \epsilon} \simeq 4 \times 10^{-5} \frac{H^2}{M_{\text{Pl}}^2} \frac{1}{r} \quad (\text{S5})$$

where we used the tensor-to-scalar ratio rather than the first slow roll parameter, using  $r = 16\epsilon$ . The ratio of the power in this isocurvature over adiabatic perturbations is then

$$\alpha_{II} \sim n^2 r \quad (\text{S6})$$

where we dropped  $\mathcal{O}(1)$  terms and used  $\bar{R} \sim M_{\text{Pl}}^2$ . We see that the Planck bound  $\alpha_{II} < 3.9 \times 10^{-2}$  is satisfied for  $n = 2$  and  $r < 10^{-2}$ , which is, for example satisfied for Starobinsky inflation, Higgs(-like) inflation and some  $\alpha$ -attractor models, where  $r = \mathcal{O}(10^{-3})$ . As the inflationary scale is lowered, this bound is more easily satisfied.

### C. Estimate of the asymmetry

We provide a more detailed derivation for the asymmetry calculation than the one found in the main text, following Refs. [55, 56]. The scalar potential for the complex field  $V(\Phi) = \lambda_\Phi |\Phi|^4 + m_\Phi^2 |\Phi|^2 - A(\Phi^2 + \Phi_*^2)$  with quadratic symmetry-breaking terms is

$$V(\Phi) = \lambda_\Phi |\Phi|^4 + m_\Phi^2 |\Phi|^2 - A(\Phi^2 + \Phi_*^2) \quad (\text{S7})$$

The field equations for the real and imaginary parts are:

$$\ddot{\phi}_R + 3H\dot{\phi}_R + m_R^2 \phi_R + \lambda_\Phi (\phi_R^2 + \phi_I^2) \phi_R = 0, \quad (\text{S8})$$

$$\ddot{\phi}_I + 3H\dot{\phi}_I + m_I^2 \phi_I + \lambda_\Phi (\phi_R^2 + \phi_I^2) \phi_I = 0, \quad (\text{S9})$$

where

$$m_R^2 = m_\Phi^2 - 2A; \quad m_I^2 = m_\Phi^2 + 2A. \quad (\text{S10})$$

while the Hubble expansion is that of a radiation-dominated Universe ( $H \propto t^{1/2}$ .)

At large field values (defined as  $|\Phi| > \phi_* = m_\Phi/\sqrt{\lambda_\Phi}$ ), the symmetry-breaking term is subleading, and we consider the dominant term of the potential

$$V(\Phi) \simeq \lambda_\Phi |\Phi|^4, \quad |\Phi| > \phi_*, \quad (\text{S11})$$

while at small field values, the quartic term is negligible, and we may approximate the potential as

$$V(\Phi) \simeq m_\Phi^2 |\Phi|^2 - A(\Phi^2 + (\Phi^*)^2), \quad |\Phi| < \phi_* \quad (\text{S12})$$

By defining time  $t_*$  as  $|\Phi(t_*)| = \phi_*$ , we approximate the field evolution during the two eras as [87]:

When  $t < t_*$ :

$$\phi_R(t < t_*) = \left(\frac{a_{in}}{a}\right) \phi_{R,in} \quad (S13)$$

$$\phi_I(t < t_*) = \left(\frac{a_{in}}{a}\right) \phi_{I,in} \quad (S14)$$

$$\phi_R(t > t_*) = \phi_{R,*} \left(\frac{a_*}{a}\right)^{3/2} \cos(m_R(t - t_*)), \quad (S15)$$

$$\phi_I(t > t_*) = \phi_{I,*} \left(\frac{a_*}{a}\right)^{3/2} \cos(m_I(t - t_*)) \quad (S16)$$

where  $\phi_{R,*} = (a_{in}/a_*)\phi_{R,in}$  and  $\phi_{I,*} = (a_{in}/a_*)\phi_{I,in}$ . The conserved charge density in the  $\Phi$  condensate is

$$n_0(t) = i \left( \Phi^\dagger \dot{\Phi} - \dot{\Phi}^\dagger \Phi \right) = \dot{\phi}_R \phi_I - \phi_R \dot{\phi}_I \quad (S17)$$

where we have used the subscript ‘0’ to denote the generated asymmetry in the  $\Phi$  sector alone, without considering the decay to SM particles.

Substituting the approximate solutions for the background fields, the asymmetry becomes

$$n_0(t) = \phi_{R,*} \phi_{I,*} \left(\frac{a_*}{a}\right)^3 [m_I \sin(m_I(t - t_*)) \cos(m_R(t - t_*)) - m_R \sin(m_R(t - t_*)) \cos(m_I(t - t_*))] . \quad (S18)$$

Since the symmetry-breaking term is subdominant to the other terms in the potential, we consider  $A \ll m_\Phi^2$  and expand the asymmetry  $n_0(t)$  at leading order in  $A/m_\Phi^2$

$$n_0(t) = m_\Phi \phi_{R,*} \phi_{I,*} \left(\frac{a_*}{a}\right)^3 \left[ \sin\left(\frac{2A(t - t_*)}{m_\Phi}\right) + \frac{A}{m_\Phi^2} \sin(2m_\Phi(t - t_*)) \right] . \quad (S19)$$

The second term is highly oscillatory and will amount to zero when averaged over several field oscillations. Hence, for  $t > t_*$  the expression in Eq. (S19) reduces to

$$n_0(t) = \phi_{R,*} \phi_{I,*} \left(\frac{\phi_{in}}{\phi_*}\right) \left(\frac{a_{in}}{a}\right)^3 m_\Phi \sin\left(\frac{2A(t - t_*)}{m_\Phi}\right) . \quad (S20)$$

The generated asymmetry will oscillate around zero with a period  $T_{\text{asy}} = \pi m_\Phi/A$ . Defining the comoving asymmetry  $n_C(t) \equiv (a(t)/a_{in})^3 n(t)$ , we can estimate the transfer of generated asymmetry to a conserved SM asymmetry via  $B$ -conserving  $\Phi$  decay to SM particles with a constant rate  $\Gamma_\Phi$ .

Finally, the transferred asymmetry to the SM can be calculated as

$$\tilde{n}_C(t) = \int_{t_*}^t dt \Gamma_\Phi n_C(t) = \frac{\Gamma_\Phi \phi_*^2 \sin(2\theta) m_\Phi}{2} \int_{t_*}^t dt e^{-\Gamma_\Phi(t-t_*)} \sin\left(\frac{2A(t - t_*)}{m_\Phi}\right) \quad (S21)$$

with  $\phi_{R,*} \phi_{I,*} = \phi_*^2 \sin\theta \cos\theta = \frac{1}{2} \phi_*^2 \sin 2\theta$ . The final expression for the transferred asymmetry for  $t - t_* \gg m_\Phi/A$  is

$$\tilde{n}_C = \frac{\Gamma_\Phi \phi_*^2 \sin(2\theta) m_\Phi^2}{2A} \left( 1 + \left( \frac{\Gamma_\Phi m_\Phi}{2A} \right)^2 \right)^{-1} . \quad (S22)$$

This expression has two limiting cases depending on whether the  $\Phi$  lifetime is short ( $\Gamma_\Phi \gg 2A/m_\Phi$ ) or long ( $\Gamma_\Phi \ll 2A/m_\Phi$ ) compared to the period of oscillation of the asymmetry:

$$\tilde{n}_C = \begin{cases} \frac{2A}{\Gamma_\Phi} \phi_*^2 \sin(2\theta) & \Gamma_\Phi \gg 2A/m_\Phi \\ \frac{\Gamma_\Phi m_\Phi^2}{2A} \phi_*^2 \sin(2\theta) & \Gamma_\Phi \ll 2A/m_\Phi \end{cases} . \quad (S23)$$

In the absence of efficient washout (as discussed in the main text and Supplemental Material Sect. D),  $\Phi$  asymmetry  $\tilde{n}_C/s$  corresponds directly to baryon or lepton number asymmetry, which we assume below for simplicity. In case

of a large washout effect,  $\tilde{n}_c/s$  would be larger than the resultant  $n_B/s$ . We do not elaborate on how the washout affects the prediction in  $n_B/s$  in the latter case, as it is highly dependent on the details of the asymmetry transfer mechanism. Instead, we will demonstrate the feasibility of generating  $\tilde{n}_c/s \gtrsim 10^{-10}$  that can compensate for a potentially large washout suppression.

Ultimately, the quantity  $n_B/s$  needs to match the observed value

$$\left. \frac{n_B}{s} \right|_{\text{obs}} = 0.861 \pm 0.005 \times 10^{-10}.$$

To this end, we multiply the comoving transferred asymmetry with  $(a_*/a)^3$  to compute the total asymmetry

$$\tilde{n} = \left( \frac{a_*}{a} \right)^3 \tilde{n}_c \quad (\text{S24})$$

For the RD universe, as in our case, the equation of state is  $w = 1/3$  leading to

$$\left( \frac{a_*}{a} \right)^3 = \left( \frac{H(t)}{H_*} \right)^{3/2} \quad (\text{S25})$$

Dividing  $\tilde{n}$  by the entropy density  $s = 4k_T^2 T^3$ , with  $k_T = \sqrt{\pi^2 g(T)/90}$ , we arrive at the baryon-to-photon ratio

$$\frac{n_B}{s} = \begin{cases} \left( \frac{4\alpha^3}{k_{T_d}^6 \lambda_\Phi} \right)^{1/4} \left( \frac{A}{m_\Phi^2} \right) \left( \frac{m_\Phi M_{\text{P}}}{T_d^2} \right) \sin(2\theta) & \Gamma_\Phi \gg 2A/m_\Phi \\ \left( \frac{\alpha^3 k_{T_d}^2}{64\lambda_\Phi} \right)^{1/4} \left( \frac{m_\Phi^2}{A} \right) \left( \frac{T_d^2}{m_\Phi M_{\text{P}}} \right) \sin(2\theta) & \Gamma_\Phi \ll 2A/m_\Phi, \end{cases} \quad (\text{S26})$$

where the  $\Phi$  decay completes when  $\Gamma_\Phi = H(T_d) = k_{T_d} T_d^2/M_{\text{P}}$  and the Hubble scale at  $t_*$  is  $H_* \simeq \frac{3}{4} m_\Phi^2/\lambda_\Phi$ . We can also elucidate the dependence on  $\phi_{\text{in}}$ , by rewriting the above expression as

$$\frac{n_B}{s} = \begin{cases} \mu \left( \frac{4\lambda_\Phi \alpha^3}{k_{T_d}^6} \right)^{1/4} \left( \frac{A}{m_\Phi^2} \right) \left( \frac{\phi_{\text{in}} M_{\text{P}}}{T_d^2} \right) \sin(2\theta) & \Gamma_\Phi \gg 2A/m_\Phi \\ \mu \left( \frac{\alpha^3 k_{T_d}^2}{64\lambda_\Phi^3} \right)^{1/4} \left( \frac{m_\Phi^2}{A} \right) \left( \frac{T_d^2}{\phi_{\text{in}} M_{\text{P}}} \right) \sin(2\theta) & \Gamma_\Phi \ll 2A/m_\Phi, \end{cases} \quad (\text{S27})$$

where for sufficient resonance, we require  $\mu^2 \equiv m_\Phi^2/(\lambda_\Phi \phi_{\text{in}}^2) \lesssim 10^{-5}$ .

In the case where the asymmetry in the  $\Phi$  field is first transferred to a SM lepton asymmetry  $n_L$ , which is later converted to a baryon asymmetry  $n_B$  via the sphaleron process, the above result gets multiplied by a factor of 28/79 since [88–90]

$$\frac{n_B}{s} = -\frac{28}{79} \frac{n_L}{s}. \quad (\text{S28})$$

Figure S1 shows the resulting asymmetry as a function of the temperature of the universe at the time of complete  $\Phi$  decay for different values of the potential parameters;  $m_\Phi$  and  $A$ . The quartic term is chosen to keep  $m_\Phi^2/\lambda_\Phi \phi_{\text{in}}^2 = 10^{-5}$  for sufficient resonance. We see the strong dependence of  $n_B/s$  on  $A$  and  $T_d$ , as expected. This allows the model to be viable, even in cases where significant washout occurs, by increasing the initially produced asymmetry through proper parameter choices.

Finally, let us reiterate one assumption that was made in the above analytic results for the generated asymmetry. As mentioned in the main text, our analysis assumes that the motion of  $\Phi$  is radial at early times, for  $\lambda_\Phi |\Phi|^4 \gg m_\Phi^2 |\Phi|^2$ . After that, the potential is dominated by the quadratic terms, which in our case includes the bare mass and the asymmetry  $A(\Phi^2 + \Phi_*^2)$ . By simply equating the quartic and bare mass terms, we arrive at the time of transition between the two regimes of  $t_*$  when  $|\Phi(t_*)| = m_\Phi/\sqrt{\lambda_\Phi}$ . Demanding that at early times (before  $t_*$ ) the asymmetry term can be neglected leads to  $\epsilon_\Phi = A/m_\Phi^2 < (\mu^2/15\alpha)(\phi_{\text{in}}^2/M_{\text{P}}^2)$  where  $\mu^2 \equiv m_\Phi^2/(\lambda_\Phi \phi_{\text{in}}^2) \lesssim 10^{-5}$ . For  $\phi_{\text{in}} \sim M_{\text{P}1}$

the above inequality can be written as  $\epsilon_\Phi \lesssim 10^{-5}$ . If we push  $\epsilon_\Phi$  above this value, the model is not invalidated, but the asymmetry would get an extra suppression factor since  $\sin \theta < \sin \theta_{\text{in}}$ . The amount of suppression depends on the amount of non-radial motion for  $t < t_*$ . That being said, the computed  $n_B/s$  can be many orders of magnitude above the measured value of  $10^{-10}$ , meaning that a suppression of  $\sin \theta$  is not “fatal” for the model, even for  $\epsilon_\Phi > 10^{-5}$ . We do not perform a detailed analysis for this regime, which simply involves computing the angular motion of  $\Phi$  from the first instant when it starts rolling for a given set of potential parameters.

As an example, for the benchmark values of  $\lambda_\Phi \sim 10^{-30}$  and  $m_\Phi = 10 \text{ GeV}$ , we must have  $\epsilon_\Phi \lesssim 10^{-6}$  for the validity of our estimates in Eq. (5). The temperature at the decay can vary between  $T_d^{\text{max}} \sim 10^8 \text{ GeV}$  for instantaneous decay and  $T_d^{\text{min}} = 10 \text{ MeV}$ , if the decay occurs right before BBN. Therefore, to obtain the correct ratio of  $n_B/s$ , we require  $\epsilon_\Phi = 10^{-38}(T_d/\text{GeV})^2$  when  $\gamma_\Phi \ll \epsilon_\Phi$ .

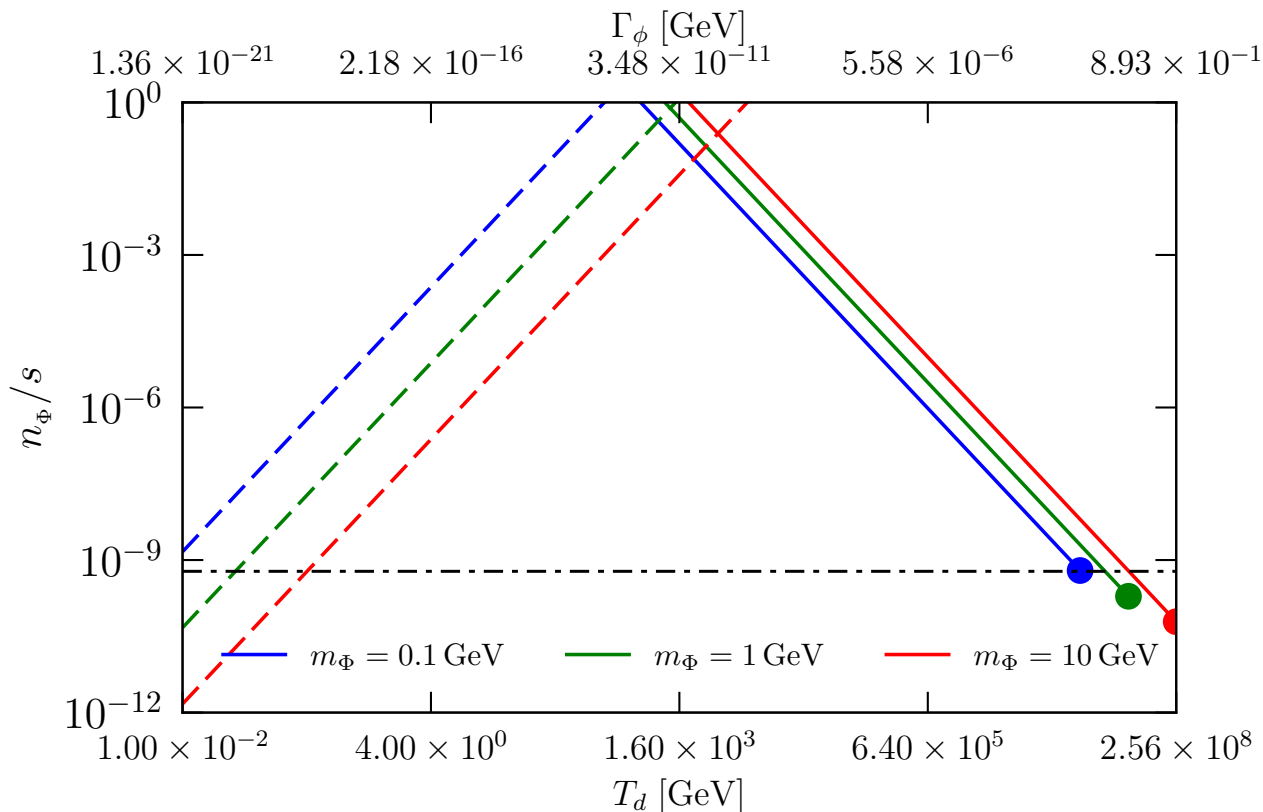


FIG. S1. The maximum baryon-to-photon ratio  $n_B/s|_{\text{max}} = n_\Phi/s$  (neglecting possible washout and the sphaleron factor) for three different masses of the scalar field as in Fig (1) as a function of the temperature  $T_d$  of the  $\Phi$  decay. The solid and dashed lines correspond to  $\epsilon_\Phi = 10^{-20}$  and  $\epsilon_\Phi = 10^{-6}$  respectively. The maximum temperature (denoted as the dots) for each line corresponds to the case of instantaneous decay of the scalar at  $t = t_*$ . The horizontal dot-dashed line corresponds to the observed value of the baryon asymmetry.

#### D. Transfer of the $\Phi$ asymmetry to the SM baryon asymmetry

In this section we elaborate the example models realizing the transfer of  $\Phi$  asymmetry to the SM baryon asymmetry and the related constraints.

(A)  $\Phi$  decay to leptons (leptogenesis).

A simple renormalizable model involves:

$$\mathcal{L} \supset y_N, {}_i\Phi\bar{N}_i^C N_i + g_\nu, {}_{ij}\bar{N}_i H L_j + \text{h.c.} \quad (\text{S29})$$

where  $N_i$ 's are right-handed (RH) Majorana right-handed neutrinos,  $H$  is SM Higgs,  $L_j$  are SM lepton doublets. The number of  $N$  species,  $N_N$ , is a model-dependent parameter, and one can take  $N = 1$  for simplicity or  $N_N = 3$  as an example by analogy to the SM neutrinos. Again, while it is appealing to simultaneously address the origin of neutrino masses, it is not imposed as a requirement for our consideration.

We consider the simple scenario where  $\Phi$  decays to  $NN$ , then  $N$  transfers the asymmetry to SM leptons via freeze-out or freeze-in processes as considered in leptogenesis literature [58–63, 91]. As seen from our GW results,  $m_\Phi \lesssim O(10)$  GeV is preferred in order to yield detectable GW frequency below  $\sim 100$  Hz. This implies that light  $N$  of mass  $\lesssim O(1 - 10)$  GeV. In this mass range, conventional  $N$  decays to SM leptons via a 3-body or loop-suppressed process, which typically occurs after electroweak sphaleron already turns off, albeit before BBN. The washout effect from inverse decay or back-scattering is also significant in this low mass range. However, as found in recent leptogenesis literature, asymmetry transfer from  $N$  to SM leptons can be realized while sphaleron is still active by freeze-out (generalized out-of-equilibrium decay or scattering) or freeze-in (via  $N$ - $\nu_{SM}$  mixing/oscillation) mechanisms, for  $m_N$  as low as  $O(100)$  MeV. The strength of the washout effect can be highly flavor-dependent. Even in the presence of large washout suppression, as shown in the main text, our Affleck-Dine model can initially generate a larger  $\Phi$  asymmetry, which compensates for the washout to eventually result in the observed baryon asymmetry. Unlike with the leptogenesis case, here, the  $NHL$  interaction only serves the purpose of transferring the  $\Phi$  ( $N$ ) asymmetry to SM leptons instead of generating the asymmetry via CP violation in the SM neutrino sector. Therefore, the details of the asymmetry evolution in our case may differ from its leptogenesis counterparts and are highly model-dependent, which may be elucidated by dedicated studies beyond the scope of this work. Furthermore, an alternative to the Majorana  $N$  as shown in Eq. S29 is to introduce quasi-Dirac  $N$  where the washout effect can be more suppressed for GeV mass range (also see [92] for this possibility and the related phenomenological implications). For all of the above possibilities for  $N$  to SM asymmetry transfer,  $\Phi \rightarrow NN$  decay is required to occur before EW sphaleron turns off, i.e.  $\Gamma_{\Phi \rightarrow NN} \sim y_\Phi^2 m_\Phi / (16\pi) \gtrsim H(T_{EW})$ . This leads to the constraint  $y_\Phi \gtrsim 10^{-7} \sqrt{\frac{\text{GeV}}{m_\Phi}}$ , which can be easily satisfied.

Laboratory signatures of the case of  $\Phi$  decaying to leptons generally relate to sterile neutrino searches in the mass range of  $O(0.1 - 10)$  GeV, which are being conducted at a range of experiments such as DUNE, SHiP, FASER et al. [41–46, 93].

(B)  $\Phi$  decay to baryons.

A simple renormalizable model in this case includes:

$$\mathcal{L} \supset y_\chi \phi_\chi \chi \chi + g_i \chi \bar{u}_i \varphi + \lambda_{ij} \varphi d_i d_j + \text{h.c.} \quad (\text{S30})$$

where  $\chi$  is a singlet Majorana fermion,  $\varphi$  is an up-type diquark scalar, and the flavor indices  $i, j = 1, 2, 3$  in down-type quark combination  $d_i d_j$  should be antisymmetric. This type of model finds its close analogy in supersymmetric theories, in particular,  $\chi$  may relate to neutralino or singlino [94],  $\varphi$  an up-type squark,  $\lambda_{ij}$  as UDD type of R-parity violating (RPV) coupling. Therefore, existing searches for RPV SUSY may lead to constraints on masses and couplings that we consider here. The LHC constraints on the colored particle  $\phi$  depend on whether it resembles the first two generations of squark or stop, and depends on whether RPV decay  $\phi \rightarrow dd$  or R-parity conserving decay  $\phi \rightarrow u\chi$  dominates (assuming  $\chi$  reveals itself as MET) [39, 95–97]. In any case, generally,  $m_\varphi \gtrsim 1$  TeV is the ballpark of the current LHC constraints, which we will use for our estimates. This constraint determines that in the parameter range of our interest where  $m_\chi \sim O(1 - 10)$  GeV,  $\chi$  decays proceeds with 3-body channel  $\chi \rightarrow udd$ . For simplicity, we assume  $g_i \sim 1$ . B-violating coupling  $\lambda_{ij}$  is subject to various constraints by laboratory searches at the intensity frontier. This model does not involve L-violation and does not induce proton decay, which usually introduces constraints on B-violating couplings [98]. Due to the antisymmetry in  $i, j$ ,  $n$ - $\bar{n}$  constraint is rather weak, while di-nucleon decay  $pp \rightarrow K^+ K^+$  provides the strongest bound [99, 100] of  $\lambda_{12} \lesssim 10^{-6}$ , for  $m_\varphi \sim \text{TeV}$ ,  $m_\chi \sim O(\text{GeV})$ . However, the bound is relaxed for heavy flavor quarks, e.g.  $\lambda_{23} \lesssim 1$ .

The kinematic condition of  $\chi$  decaying to baryons leads to lower limit on masses:  $m_\Phi > 2$  GeV,  $m_\chi > 1$  GeV. The decays of both  $\Phi \rightarrow \chi\chi$  and  $\chi \rightarrow udd$  are required to occur before BBN, i.e.,  $\Gamma_{\Phi \rightarrow \chi\chi} \sim \frac{1}{16\pi} y_\chi^2 m_\Phi > H(T_{\text{BBN}})$ , and  $\Gamma_{\chi \rightarrow udd} > H(T_{\text{BBN}})$ . We then estimate the constraint on coupling parameters as:  $y_\chi \gtrsim 10^{-12} \frac{\text{GeV}}{m_\Phi}$ ,  $\sum_{i,j} g_i \lambda_{ij} \gtrsim$

$\sqrt{10^{-21} \frac{m_\Phi^4 \text{GeV}}{m_\chi^5}}$ . With  $m_\varphi \sim \text{TeV}$ ,  $m_\chi \sim O(\text{GeV})$ , we find that  $\sum_{i,j} g_i \lambda_{ij} \gtrsim 10^{-5}$ . If  $\lambda_{12}$  dominates  $\chi$  decay, this would

contradict the aforementioned di-nucleon decay bound. Therefore, we choose to consider the pattern of heavy flavor domination, which is well motivated and has been widely considered in SUSY context [61, 101–103]. In particular, we consider the dominant decay of  $\chi$  involves b-quark  $\chi \rightarrow udb$  or  $\chi \rightarrow usb$ . As  $m_b \simeq 4$  GeV, the kinematics requires  $m_\chi > 4$  GeV and  $m_\Phi > 8$  GeV. The involvement of heavy b-quark also alleviates the potential washout suppression of baryon asymmetry due to inverse decay  $udd \rightarrow \chi$  and back-scattering  $udd \rightarrow \bar{u}\bar{d}\bar{d}$ : by requiring  $\chi$  decay below  $T \sim m_b$  (compatible with the condition of decay before BBN), the washout effect gets Boltzmann suppression and quickly becomes inefficient.

Laboratory signatures of the case of  $\Phi$  decaying to baryons depend on model details. One interesting possibility is a multi-jet signal at the LHC (eight jets with b-tagging), potentially with displaced vertices, from pair-production of  $\phi$  followed by  $\phi \rightarrow \chi u \rightarrow uudd$ , which is distinct yet relates to existing searches such as [40].

## E. Asymmetry dependence of GW production

It is worth exploring in more detail the connection between the asymmetry of the potential and the shape and amplitude of the resulting GW spectrum. Let us start from the symmetric case  $A = 0$ , where the potential becomes

$$V(\phi_R, \phi_I) = \frac{1}{4}\lambda_\Phi(\phi_R^2 + \phi_I^2)^2 + \frac{1}{2}m_\Phi^2(\phi_R^2 + \phi_I^2) = \frac{1}{4}\lambda_\Phi\phi_R^4 + \frac{1}{4}\lambda_\Phi\phi_I^4 + \frac{1}{2}m_\Phi^2\phi_R^2 + \frac{1}{2}m_\Phi^2\phi_I^2 + \frac{1}{2}\lambda_\Phi\phi_R^2\phi_I^2 \quad (\text{S31})$$

Since the potential is radially symmetric, we can redefine the fields as  $\phi_\parallel = \phi_R \cos\theta - \phi_I \sin\theta$  and  $\phi_\perp = \phi_R \sin\theta + \phi_I \cos\theta$ , where at the background level  $\phi_\perp = 0$ . This essentially makes the analysis follow our earlier work [48], where we considered (among others) systems with two scalar fields with a quartic coupling, where one field is initially displaced from its minimum, and the other is (classically) at zero. This specific example is a combination of Models A and D of Ref. [48]. The equations of motion for the fluctuations in the  $\phi_\parallel - \phi_\perp$  basis are

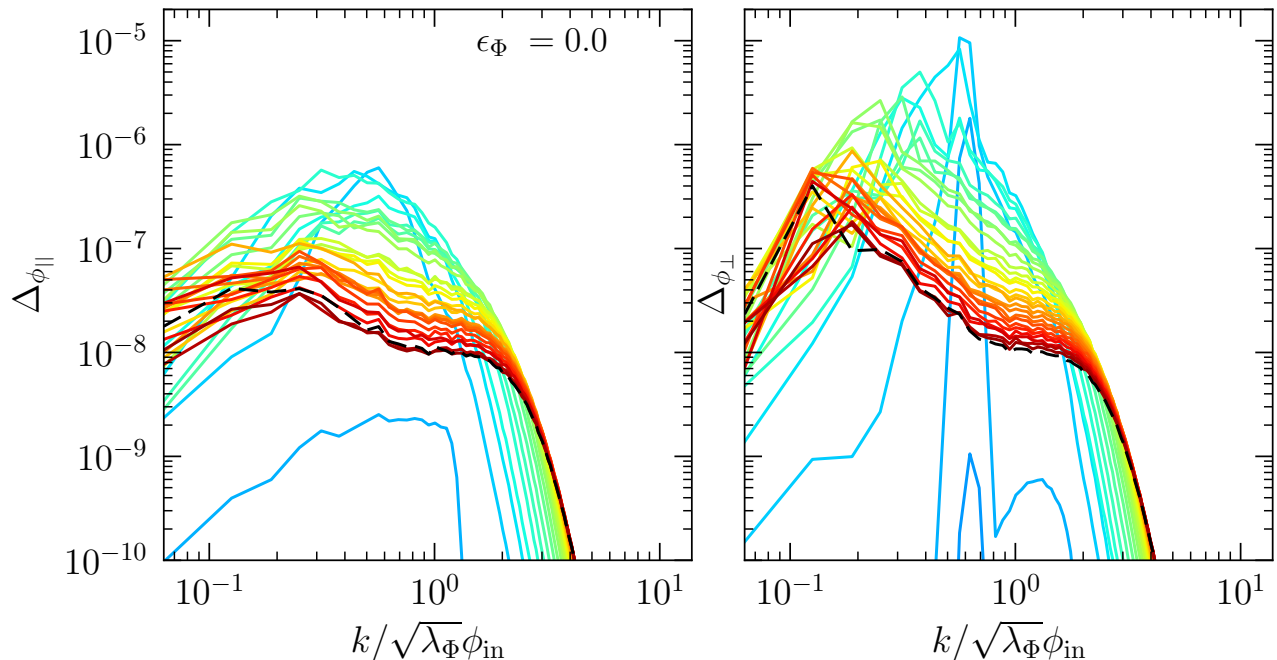


FIG. S2. The spectra of the scalar field fluctuations along (left) and perpendicular (right) to the direction of the background trajectory in the case of a rotationally symmetric potential with  $A = 0$ ,  $\lambda_\Phi = 5 \times 10^{-35}$  and  $m_\Phi = 0.1$  GeV.

$$\delta\ddot{\phi}_{\parallel} + 3H\delta\dot{\phi}_{\parallel} + \left(\frac{k^2}{a^2} + m_{\Phi}^2 + 3\lambda_{\Phi}\bar{\phi}^2\right)\delta\phi_{\parallel} = 0 \quad (\text{S32})$$

$$\delta\ddot{\phi}_{\perp} + 3H\delta\dot{\phi}_{\perp} + \left(\frac{k^2}{a^2} + m_{\Phi}^2 + \lambda_{\Phi}\bar{\phi}^2\right)\delta\phi_{\perp} = 0 \quad (\text{S33})$$

In principle, we can see two sources of parametric resonance: self-resonance of the  $\phi_{\parallel}$  field due to the quartic term  $3\lambda_{\Phi}\bar{\phi}^2\delta\phi_{\parallel}$  and resonant amplification of the  $\phi_{\perp}$  field through the coupling term  $\lambda_{\Phi}\bar{\phi}^2\delta\phi_{\perp}$ .

The background field trajectory is (by construction) along  $\bar{\phi}_{\perp} = 0$  and thus a straight line through the origin on the  $\phi_R - \phi_I$  plane. Floquet analysis of a quartic field in a nonexpanding universe predicts that the resonance is stronger for  $q = 1$  ( $\mu_k^{max} \sim 0.15$ ) than  $q = 3$  ( $\mu_k^{max} \sim 0.04$ ) [67], where  $q$  is defined as the coefficient before  $\lambda_{\Phi}\bar{\phi}^2$  in Eqs. S33. Figure S2 shows the spectra of  $\delta\phi_{\parallel}, \delta\phi_{\perp}$  for different times, where we see that the  $\delta\phi_{\perp}$  spectrum dominates, as expected from the standard analysis of preheating of quartic fields [67]. In the  $\phi_R - \phi_I$  basis, the spectra will be identical for  $\theta = \pi/4$ , since each spectrum has an equal contribution from  $\delta\phi_{\parallel}$  and  $\delta\phi_{\perp}$ . If the initial angle between the real and imaginary parts of  $\Phi$  changes, the spectra of  $\delta\phi_{\parallel}$  and  $\delta\phi_{\perp}$  remain unchanged, whereas the spectra of  $\phi_R$  and  $\phi_I$  change, since the inner product between the basis vectors of the two bases change with the angle  $\theta$ . That being said, the resulting GW spectrum is unchanged, as expected, due to the rotational symmetry of the potential.

We now move to the case of  $A \neq 0$ . We parametrize the effect by  $\epsilon_{\Phi} = A/m_{\Phi}^2$ . As expected, small values of the angle do not significantly affect the background trajectory and the resonance structure. As seen in Fig. S3, for  $\epsilon_{\Phi} \leq 0.005$ , the GW spectrum is independent of the initial angle  $\theta_{\text{in}}$  and actually indistinguishable from the symmetric case with  $\epsilon_{\Phi} = 0$ . This means that for the asymmetry values that we use for our benchmark examples  $\epsilon_{\Phi} < 10^{-5}$ , the resonance is “blind” with respect to the exact value of asymmetry in the potential. That being said, it is worth

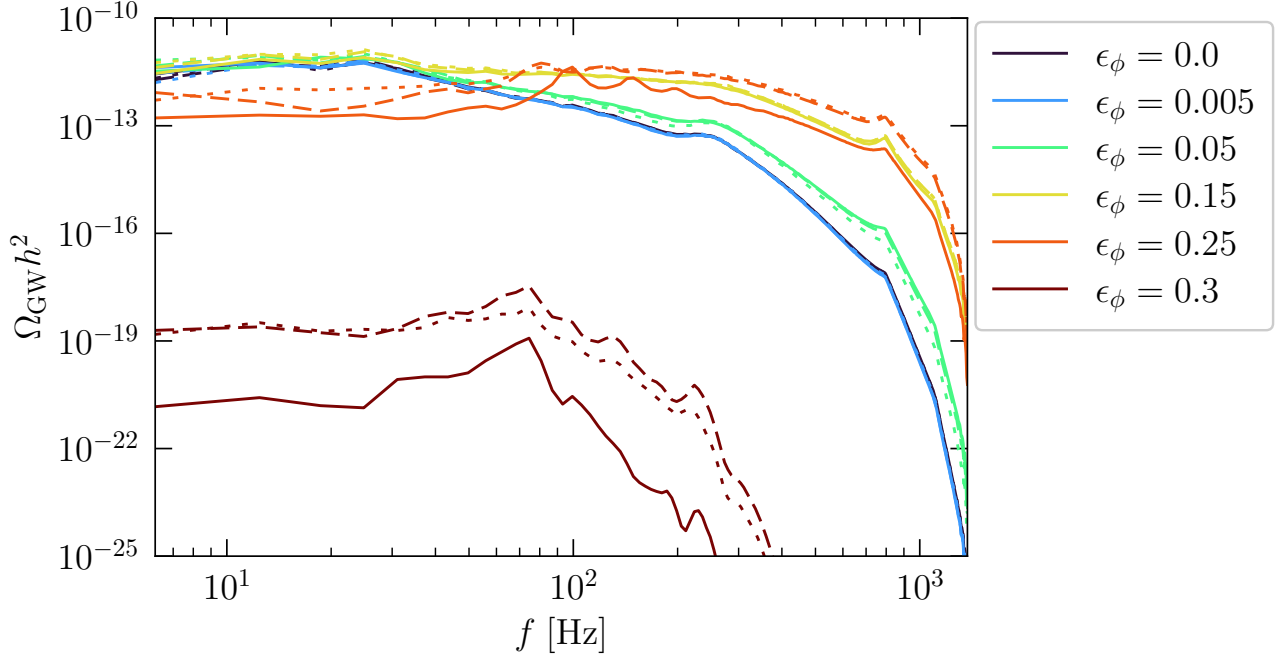


FIG. S3. The resulting GW spectra for different values of the asymmetry parameter  $A$  (color-coded according to the legend) and initial angle  $\theta \equiv \arctan(\phi_I/\phi_R)|_{\text{init}} = \pi/6, \pi/4, \pi/3$  (solid, dashed and dotted respectively).

pushing the asymmetry value higher in order to cover the entire possible parameter space. For  $0.05 \lesssim \epsilon_{\Phi} \lesssim 0.15$  we see an enhancement of the GW spectrum at large values of the frequency  $f \gtrsim 100$  Hz, while the independence of  $\theta_{\text{in}}$  still holds. This is an intriguing observation, as it provides an additional motivation for GW detectors that can probe frequencies around 1 kHz with a sensitivity similar to CE and ET [104, 105]. For  $\epsilon_{\Phi} \simeq 0.25$  the UV enhancement of the GW spectrum remains, but we also see a difference between the initial angle choices between the real and imaginary



parts of  $\Phi$ . This means that a possible detection of a spectrum with such a UV enhancement would suffer from a partial degeneracy between  $\epsilon_\phi$  and  $\theta_{\text{in}}$ . Since we focused on  $\epsilon_\phi \ll 1$ , such a highly model-dependent calculation is outside the scope of the present work. Finally, for  $\epsilon_\phi \gtrsim 0.3$ , parametric resonance is severely suppressed, rendering the GW signals below the detection threshold.